

Synthesis, Structure, and Reactivity of Rhodium and Iridium Complexes of the Chelating Bis-Sulfoxide *t*BuSOC₂H₄SO*t*Bu. Selective O–H Activation of 2-Hydroxy-*isopropyl*-pyridine

Thomas Schaub,[†] Yael Diskin-Posner,[‡] Udo Radius,[§] and David Milstein^{*†}

Departments of Organic Chemistry and Unit of Chemical Research Support, The Weizmann Institute of Science, Rehovot 76100, Israel, and Institute for Inorganic Chemistry, University of Karlsruhe, 76131 Karlsruhe, Germany

Received February 29, 2008

The chloro-bridged rhodium and iridium complexes [M₂(BTSE)₂Cl₂] (M = Rh **1**, Ir **2**) bearing the chelating bis-sulfoxide *t*BuSOC₂H₄SO*t*Bu (BTSE) were prepared by the reaction of [M₂(COE)₄Cl₂] (M = Rh, Ir; COE = cyclooctene) with an excess of a racemic mixture of the ligand. The cationic compounds [M(BTSE)₂][PF₆] (M = Rh **3**, Ir **4**), bearing one S- and one O-bonded sulfoxide, were also obtained in good yields. The chloro-bridges in **2** can be cleaved with 2-methyl-6-pyridinemethanol and 2-aminomethyl pyridine, resulting in the iridium(I) complexes [Ir(BTSE)(Py)(Cl)] (Py = 2-methyl-6-pyridinemethanol **5**, 2-aminomethyl-pyridine **6**). In case of the bulky 2-hydroxy-*isopropyl*-pyridine, selective OH oxidative addition took place, forming the Ir(III)-hydride [Ir(BTSE)(2-*isopropoxy*-pyridine)(H)(Cl)] **7**, with no competition from the six properly oriented C–H bonds. The cationic rhodium(I) and iridium(I) compounds [M(BTSE)(2-aminomethyl-pyridine)][X] (M = Rh **8**, Ir **10**), [Rh(BTSE)(2-hydroxy-*isopropyl*-pyridine)][X] **9** (stabilized by intramolecular hydrogen bonding), [Ir(BTSE)(pyridine)₂][PF₆] **12**, [Ir(BTSE)(α -picoline)₂][PF₆] **13**, and [Rh(BTSE)(1,10-phenanthroline)][PF₆] **14** were prepared either by chloride abstraction from the dimeric precursors or by replacement of the labile oxygen bonded sulfoxide in **3** or **4**. Complex **14** exhibits a dimeric structure in the solid state by π – π stacking of the phenanthroline ligands.

Introduction

Sulfoxides are air stable, nontoxic, and well-studied ligands in transition-metal chemistry. They exhibit versatile coordination behavior and can coordinate either via the sulfur or oxygen atoms according to electronic and steric demands.¹ Sulfoxide complexes have been introduced successfully in homogeneous catalysis for various transformations.² Some years ago, our group described the synthesis and reactivity of the first structurally characterized Rh(I)^{3,4} and Ir(I) DMSO^{4,5} complexes, and the oxidative addition of water and methanol by the iridium compounds, a process observed before with late transition metal complexes bearing phosphine ligands.⁶ Because of insufficient stability of the Rh(I) and Ir(I) DMSO complexes as catalysts in aqueous media,⁷ we are interested in the use of chelating bis-sulfoxides, which

could enhance the stability of the complexes. Complexes of chelating bis-sulfoxides, which are known since the late 1960s,⁸ are mainly described for ruthenium,^{9,11a} platinum,^{8,10} palladium,^{2m,n,8,9b,10d,11} silver,¹² and the lanthanides,^{12b,13} whereas just a few examples are known for rhodium^{2o,10d,11a,b} and iridium.^{10d} The reactivity of these rhodium and iridium compounds was not described, with the exception of a very recently reported rhodium complex bearing a chiral bis-sulfoxide, which was an excellent catalyst in asymmetric synthesis.^{2o}

Results and Discussion

Ligand Synthesis. We focused our work on the bis-sulfoxide *rac*-1,2-bis(*tert*-butylsulfinyl)ethane (*t*BuSOC₂H₄SO-*t*Bu, BTSE) as a sterically demanding chelating ligand, which was prepared in moderate yields in a simple two step synthesis (Scheme 1).

In the first step, 1,2-bis(*tert*-butylthio)ethane was prepared by the reaction of 1,2-dibromoethane with K*S**t*Bu and then oxidized to BTSE with hydrogen peroxide in methanol. The

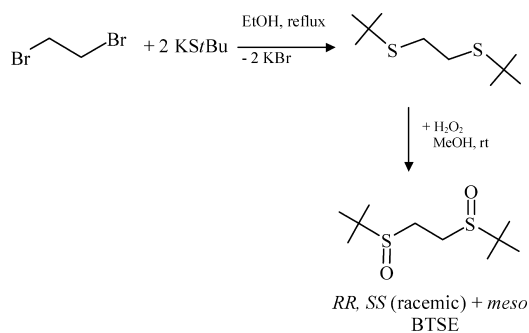
* To whom correspondence should be addressed. E-mail: david.milstein@weizmann.ac.il.

[†] Department of Organic Chemistry, The Weizmann Institute of Science,

[‡] Department of Chemical Services, The Weizmann Institute of Science,

[§] Institute for Inorganic Chemistry, University of Karlsruhe.

Scheme 1



BTSE ligand was obtained as a mixture of the *meso*-isomer and the *RR/SS* pair in a 17:83 ratio (although the synthesis of the enantiomerically pure *RR* and *RS* isomers is known,^{9b,14} the isomeric mixture of the ligand is sufficient for first reactivity studies).

Synthesis and Characterization of BTSE Rhodium and Iridium Complexes. The COE precursors $[M_2(\text{COE})_4\text{Cl}_2]$ ($M = \text{Rh}, \text{Ir}$; COE = cyclooctene) react cleanly with an excess of the BTSE isomeric mixture to give the corresponding chloro-bridged BTSE complexes $[M_2(\text{BTSE})_2\text{Cl}_2]$ ($M = \text{Rh}$ **1**, Ir **2**) in good to moderate yields (Scheme 2).

The ^1H NMR spectra of **1** and **2** show two multiplets for the CH_2 protons in the backbone of the BTSE ligand with an integration ratio of 2:2, which indicates that just the *RR/SS* pair is coordinated to the metal and not the *meso* isomer (formation of complexes containing *meso* BTSE is avoided by using an excess of the BTSE isomeric mixture). Because of the sterically demanding *t*butyl substituents, the *RR/SS* BTSE seems to be a better ligand than the *meso* isomer, where these groups have to be located on the same side of the coordinated ligand. The IR spectra of **1** and **2** exhibit the SO stretch as a strong band at 1072 cm^{-1} in both complexes, compared to 1038 cm^{-1} in free BTSE, which is in accordance with the expected sulfur (rather than oxygen) coordination of the sulfoxide ligand.^{1b} The molecular structures of the dimers **1** and **2** were confirmed by X-ray diffraction studies on single crystals obtained by diffusion of pentane (or layering with pentane) into CH_2Cl_2 solutions of **1** and **2**. The metal atoms in **1** and **2** are located in a distorted square plane comprising BTSE and two bridging chloride ligands (Figure 1).

The *rac*-BTSE is coordinated to the metal atoms in **1** and **2** via the sulfur atoms, forming five-membered rings with $\text{L}-\text{M}-\text{L}$ angles between $87.90(7)$ and $90.08(6)^\circ$.

The cationic, all-BTSE stabilized rhodium(I) and iridium(I) complexes $[M(\text{BTSE})_2][\text{PF}_6]$ ($M = \text{Rh}$ **3**, Ir **4**) were prepared by the reaction of the corresponding $[M(\text{COE})_2(\text{O}=\text{CMe}_2)_2][\text{PF}_6]$ precursors with an excess of BTSE in CH_2Cl_2 (Scheme 3).

The CH_2 protons of the ligand backbone were detected in the ^1H NMR spectrum of **3** as four multiplets at 2.50, 3.02, 3.30, and 3.41 ppm with an integration ratio of 2:2:2:2 and in the case of **4** as three multiplets at 2.23, 3.12, and 3.34 ppm in a ratio of 2:2:4. Two sets of singlets were observed for the *t*Bu- CH_3 groups. This implies the presence of two

BTSE ligands in different coordination modes. The SO stretches in **3**(**4**) appear at 936 cm^{-1} (919 cm^{-1}) and 1072 cm^{-1} (1081 cm^{-1}), which is a clear indication for *S*- and *O*-bonding of the sulfoxide. As in the cases of **1** and **2**, coordination of the *meso* BTSE was not observed. The molecular structure of **3** was obtained by X-ray diffraction on single crystals grown by slow diffusion of diethylether into an acetone solution. The rhodium atom in **3** is centered in a distorted square-planar geometry comprised of two BTSE ligands, one coordinated via the sulfur atoms, and another via the oxygen atoms (Figure 2).

The chelating ligands form five-membered (*S*-coordinated-) and seven-membered (*O*-coordinated-) rings, which at first sight seems unusual for the same ligand, but it is in line with the structure of the DMSO complex $[\text{Rh}(\text{DMSO})_2(\text{DMSO})_2][\text{PF}_6]$,^{3,4} which bears *S*- and *O*-bound DMSO ligands trans to each other due to the strong trans effect of the sulfur-bound DMSO. Steric constraints imposed by the bulky *t*Bu substituents also play an important role in the formation of this coordination motif. To the best of our knowledge, **3** is the first example of a structurally characterized monomeric transition-metal complex with an *O*-coordinated chelating bis-sulfoxide. This coordination mode was reported before only in the case of lanthanide bis-sulfoxide compounds, in which *O*-bonding is strongly preferred due to the oxophilic nature of the lanthanides.^{12b,13}

Reactivity of the Chloro-Bridged Rhodium- and Iridium-BTSE Complexes. Although oxidative addition of water was observed in the case of the sulfoxide complexes $[\text{Ir}(\text{DMSO})_3\text{Cl}]$, $[\text{Ir}_2(\text{DMSO})_4(\text{Cl})_2]$, and $[\text{Ir}(\text{DMSO})_2(\text{DMSO})_2][\text{PF}_6]$,^{4,5} **1** and **2** did not exhibit analogous reactivity. Treatment of acetone or CH_2Cl_2 solutions of (the water-insoluble) **1** and **2** with water did not result in products of water oxidative addition. Attempts to cleave the chloro bridges of $[\text{Rh}_2(\text{BTSE})_2\text{Cl}_2]$ **1** by dissolution in pyridine-*d*₅ or DMSO-*d*₆ led, upon standing overnight at room temperature, to complete displacement of the BTSE ligand by pyridine or DMSO with the formation of $[\text{Rh}(\text{Py})_3\text{Cl}]$ and $[\text{Rh}(\text{DMSO})_3\text{Cl}]$.¹⁵ In contrast, the use of stoichiometric

- (1) (a) Alessio, E. *Chem. Rev.* **2004**, *104*, 4203. (b) Calligaris, M. *Coord. Chem. Rev.* **2004**, *248*, 351.
- (2) (a) Haddad, Y. M. Y.; Henbest, H. B.; Trocha-Grimshaw, J. *J. Chem. Soc., Perkin Trans. 1* **1974**, 592. (b) Haddad, Y. M. Y.; Henbest, H. B.; Husbands, J.; Mitchell, T. R. B.; Trocha-Grimshaw, J. *J. Chem. Soc., Perkin Trans. 1* **1974**, 596. (c) Henbest, H. B.; Trocha-Grimshaw, J. *J. Chem. Soc., Perkin Trans. 1* **1974**, 607. (d) James, B. R.; Morris, R. H. *J. Chem. Soc., Chem. Commun.* **1978**, 929. (e) Greenberg, H.; Gogoll, A.; Bäckvall, J.-E. *J. Org. Chem.* **1991**, *56*, 5808. (f) Allen, J. V.; Bower, J. F.; Williams, J. M. *J. Tetrahedron Asymmetry* **1994**, *5*, 1895. (g) Larock, R. C.; Hightower, R.; Hasvold, L. A.; Peterson, K. P. *J. Org. Chem.* **1996**, *61*, 3584. (h) Hiroi, K.; Suzuki, Y. *Tetrahedron Lett.* **1998**, *39*, 6499. (i) Hiroi, K.; Suzuki, Y.; Abe, I.; Hasegawa, Y.; Suzuki, K. *Tetrahedron Asymmetry* **1998**, *9*, 3797. (j) Petra, D. G. I.; Kamer, P. C. J.; Spek, A. L.; Schoemaker, H. E.; van Leeuwen, P. W. N. M. *J. Org. Chem.* **2000**, *65*, 3010. (k) Hiroi, K.; Suzuki, Y.; Abe, I.; Kawagishi, R. *Tetrahedron* **2000**, *56*, 4701. (l) Hiroi, K.; Izawa, I.; Takizawa, T.; Kawai, K. *Tetrahedron* **2004**, *60*, 2155. (m) Chen, M. S.; White, M. C. *J. Am. Chem. Soc.* **2004**, *126*, 1346. (n) Fraunhoffer, K. J.; Prabakaran, N.; Sirois, L. E.; White, M. C. *J. Am. Chem. Soc.* **2005**, *128*, 9032. (o) Mariz, R.; Luan, X.; Gatti, M.; Linden, A.; Dorta, R. *J. Am. Chem. Soc.* **2008**, *130*, 2172.
- (3) Dorta, R.; Rozenberg, H.; Milstein, D. *Chem. Commun.* **2002**, 710.
- (4) Dorta, R.; Rozenberg, H.; Shimon, L. J. W.; Milstein, D. *Chem.—Eur. J.* **2003**, *9*, 5237.

Scheme 2

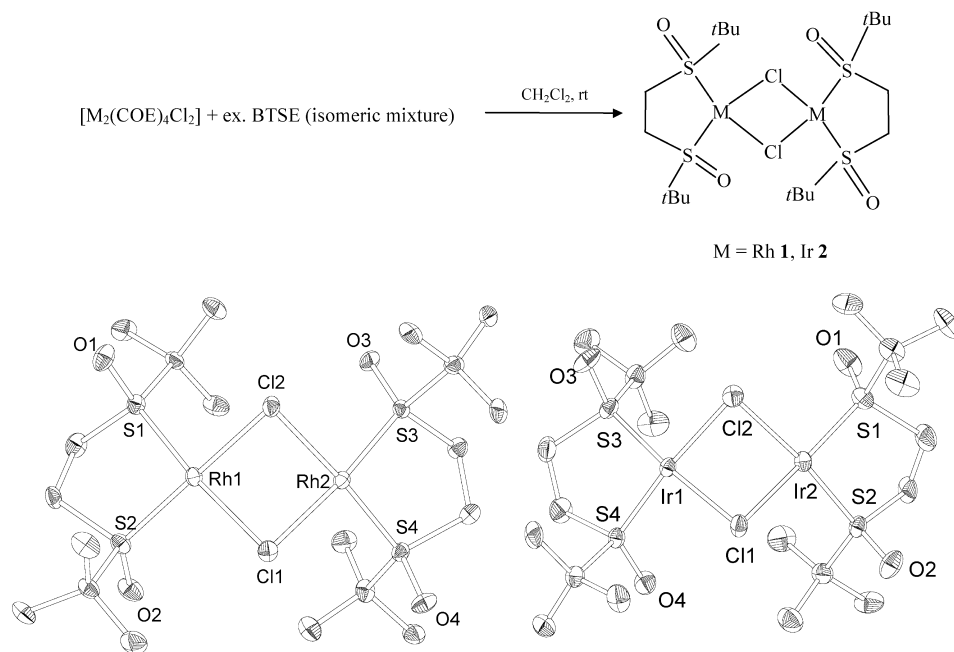
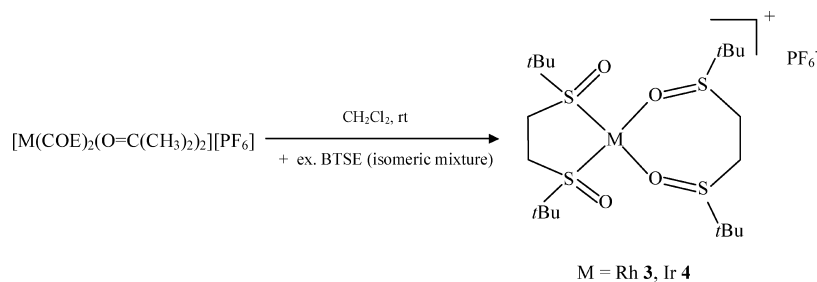


Figure 1. Thermal ellipsoid drawing of $[\text{Rh}_2(\text{BTSE})_2\text{Cl}_2]$ **1** and $[\text{Ir}_2(\text{BTSE})_2\text{Cl}_2]$ **2** at 50% probability; hydrogen atoms are omitted for clarity. Selected bond distances [Å] and angles [deg]: **1**: Rh1–Cl1 2.391(2), Rh1–Cl2 2.387(2), Rh2–Cl1 2.395(2), Rh2–Cl2 2.391(1), Rh1–Rh2 3.161(1), Rh1–S1 2.194(2), Rh1–S2 2.189(2), Rh2–S3 2.177(2), Rh2–S4 2.173(1), S1–O1 1.482(5), S2–O2 1.485(6), S3–O3 1.484(5), S4–O4 1.470(7); Cl1–Rh1–Cl2 81.26(6), S1–Rh1–S2 87.90(7), S1–Rh1–Cl2 95.17(7), S2–Rh1–Cl1 96.37(7), Cl1–Rh2–Cl2 81.10(6), S3–Rh2–S4 89.98(7), S3–Rh2–Cl2 93.85(7), S4–Rh2–Cl1 94.99(7), Rh1–Cl1–Rh2 82.68(6), Rh1–Cl2–Rh2 82.84(6). **2**: Ir1–Cl1 2.389(1), Ir1–Cl2 2.391(2), Ir2–Cl1 2.394(2), Ir2–Cl2 2.394(2), Ir1–Ir2 3.189(1), Ir1–S3 2.165(1), Ir1–S4 2.166(2), Ir2–S1 2.176(2), Ir2–S2 2.178(2), S1–O1 1.465(6), S2–O2 1.474(4), S3–O3 1.468(5), S4–O4 1.469(5); Cl1–Ir1–Cl2 79.84(5), S3–Ir1–S4 90.08(6), S3–Ir1–Cl2 95.42(6), S4–Ir1–Cl1 94.58(5), Cl1–Ir2–Cl2 79.93(5), S1–Ir2–S2 88.03(6), S1–Ir2–Cl2 96.86(6), S2–Ir2–Cl1 95.72(6), Ir1–Cl2–Ir2 83.57(5), Ir1–Cl1–Ir2 83.91(5).

Scheme 3



amounts of pyridine derivatives led to more useful reactions. We chose pyridines with different substituents in the 2- and 6-positions, including $-\text{CH}_3$, $-\text{CH}_2\text{NH}_2$, $-\text{CH}_2\text{OH}$, $-\text{C}(\text{CH}_3)_2\text{OH}$, to promote activation of the X–H bonds (X = C, N, O) by precoordination of the pyridinic substrate. In addition, the activation products are expected to be thermodynamically stabilized by chelation. It was also of interest to see if selective O–H bond oxidative addition can be observed in the presence of competing C–H bonds.

Chloro-bridge cleavage of **2** by 2-methyl-6-pyridinemethanol and 2-amino-methyl-pyridine (Scheme 4) resulted in the corresponding monomeric iridium(I) complexes $[\text{Ir}(\text{BTSE})(2\text{-methyl-6-pyridinemethanol})(\text{Cl})]$ **5** and $[\text{Ir}(\text{BTSE})(2\text{-amino-methyl-pyridine})(\text{Cl})]$ **6**. No insertion of the metal atom in CH–, OH– (both groups present in the substrate 2-methyl-6-pyridinemethanol), or NH-bonds of these two substrates was observed.

The ^1H NMR spectrum of **5** exhibits the *t*Bu protons of the BTSE ligand as two singlets, and the backbone protons as two multiplets, due to the unsymmetric nature of the complex. The resonances of the benzylic protons of the pyridine ligand were observed as two doublets at 4.75 and 6.31 ppm and the OH protons as a broad singlet at 5.16 ppm, indicating no intramolecular hydrogen bonding involving the sulfoxide oxygen.¹⁶ The SO-stretch appears in the IR spectrum as a strong band at 1064 cm^{-1} , typical for S-bonding, and the OH-stretch was detected as a strong, broad band at 3387 cm^{-1} , indicating the absence of an intramolecular hydrogen bond.¹⁷ The molecular structure of **5**, determined by an X-ray diffraction study of yellow crystals obtained by layering an CH_2Cl_2 solution of **5** with pentane, is in accord with the above-mentioned conclusions (Figure 3).

(5) Dorta, R.; Rozenberg, H.; Shimon, L. J. W.; Milstein, D. *J. Am. Chem. Soc.* **2002**, *124*, 188.

The aromatic ring of the 2-methyl-6-pyridinemethanol ligand is orientated orthogonally to the plane spanning through the iridium atom and the coordinated sulfur-, chloro- and nitrogen atoms. The OH group is directed away from the sulfoxide oxygen, confirming the absence of an intramolecular hydrogen bond.

In contrast to **5**, the ^1H NMR spectrum of **6** indicates the presence of an intramolecular hydrogen bond between one

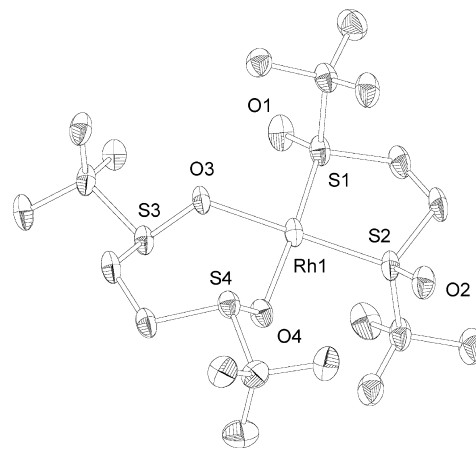
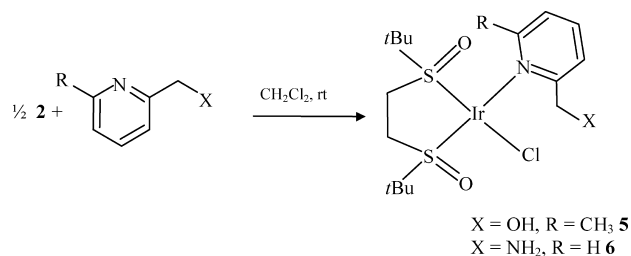


Figure 2. Thermal ellipsoid drawing of the molecular cation of $[\text{Rh}(\text{BTSE})_2][\text{PF}_6]$ **3** at 50% probability; hydrogen atoms are omitted for clarity. Selected bond distances [Å] and angles [deg]: Rh1–S1 2.163(2), Rh1–S2 2.163(2), Rh1–O3 2.104(4), Rh1–O4 2.113(4), S1–O1 1.477(4), S2–O2 1.474(4), S3–O3 1.547(4), S4–O4 1.540(4); S1–Rh1–S2 89.83(6), O3–Rh1–O4 83.87(15), O3–Rh1–S1 92.98(12), O4–Rh1–S2 93.65(11), O3–Rh1–S2 174.53(11), O4–Rh1–S1 174.79(13).

Scheme 4



NH₂ proton and BTSE. The resonances of the NH₂ protons were detected as a broad singlet at 4.90 ppm and a drastic downfield-shifted broad singlet at 8.24 ppm due to hydrogen bonding.¹⁶ The NH₂ stretch of **6** was observed as one broadband at 3217 cm⁻¹, which is also in agreement with the presence of a hydrogen bond (two bands are expected in the absence of hydrogen bonding).^{17,18}

Different reactivity was observed when the sterically more demanding pyridine-alcohol 2-hydroxy-*isopropyl*-pyridine was used. Upon reaction with **2** in methylene chloride, the OH bond underwent quantitative oxidative addition, resulting in the hydrido-alkoxy iridium(III) **7** (Scheme 5). Interestingly, the reaction is selective and no competing C–H activation was observed, despite the presence of properly oriented six C–H bonds of the methyl groups. Because cleavage of the strongest X–H (X = O, C) bond of the substrate is usually expected to lead to the strongest M–X bond,¹⁹ and because the OH bond dissociation energy in 2-hydroxy-*isopropyl*-

- (6) (a) Cole-Hamilton, D. J.; Wilkinson, G. *Nouv. J. Chim.* **1977**, *1*, 141. (b) Yoshida, T.; Matsuda, T.; Okano, T.; Otsuka, S. *J. Am. Chem. Soc.* **1979**, *101*, 2027. (c) Gotzig, J.; Werner, R.; Werner, H. *J. Organomet. Chem.* **1985**, *290*, 99. (d) Paonessa, R. S.; Prignano, A. L.; Trogler, W. C. *Organometallics* **1985**, *4*, 647. (e) Milstein, D.; Calabrese, J. C.; Williams, I. D. *J. Am. Chem. Soc.* **1986**, *108*, 6387. (f) Sponsler, M. B.; Weiller, B. H.; Stoutland, P. O.; Bergman, R. G. *J. Am. Chem. Soc.* **1989**, *111*, 6841. (g) Stevens, R. C.; Bau, R.; Milstein, D.; Blum, O.; Koetzle, T. *J. Chem. Soc., Dalton Trans.* **1990**, 1429. (h) Werner, H.; Michenfelder, A.; Schulz, M. *Angew. Chem.* **1991**, *103*, 555. *Angew. Chem., Int. Ed. Engl.* **1991**, *30*, 96. (i) Ladipo, F. T.; Kooti, M.; Merola, J. S. *Inorg. Chem.* **1993**, *32*, 1681. (j) Burn, M. J.; Fickes, M. G.; Hartwig, J. F.; Hollander, F. J.; Bergman, R. G. *J. Am. Chem. Soc.* **1993**, *115*, 5875. (k) Blum, O.; Milstein, D. *Angew. Chem.* **1995**, *107*, 210. *Angew. Chem., Int. Ed. Engl.* **1995**, *34*, 229. (l) Dorta, R.; Togni, A. *Organometallics* **1998**, *17*, 3423. (m) Tani, K.; Iseki, A.; Yamagata, T. *Angew. Chem.* **1998**, *110*, 3590. *Angew. Chem., Int. Ed. Engl.* **1998**, *37*, 3381. (n) Morales-Morales, D.; Lee, D. W.; Wang, Z.; Jensen, C. M. *Organometallics* **2001**, *20*, 1144. (o) Blum, O.; Milstein, D. *J. Am. Chem. Soc.* **2002**, *124*, 11456.
- (7) Attempts to develop catalytic reactions of unsaturated compounds such as olefins, alkynes, aldehydes, nitriles, or ketones with water in aqueous media using $[\text{Rh}(\text{DMSO})_3\text{Cl}]$ and $[\text{Ir}(\text{DMSO})_3\text{Cl}]$ as catalysts did not succeed due to the instability of these complexes under these conditions, forming elemental metals; T. Schaub, D. Milstein, unpublished results.
- (8) Madan, K.; Hull, C. M.; Herman, L. *J. Inorg. Chem.* **1968**, *7*, 491.
- (9) (a) Yapp, D. T. T.; Rettig, S. J.; James, B. R.; Skov, K. A. *Inorg. Chem.* **1997**, *36*, 5635. (b) Khair, N.; Araújo, C. S.; Alcludia, F.; Fernández, I. *J. Org. Chem.* **2002**, *67*, 345. (c) Wu, A.; Kennedy, D. C.; Patrick, B. O.; James, B. R. *Inorg. Chem. Commun.* **2003**, *6*, 996. (d) Huxham, L. A.; Cheu, E. L. S.; Patrick, B. O.; James, B. R. *Inorg. Chim. Acta* **2003**, *352*, 238. (e) Wu, A.; Kennedy, D. C.; Patrick, B. O.; James, B. R. *Inorg. Chem.* **2003**, *42*, 7579.
- (10) (a) Cattalini, L.; Michelon, G.; Marangoni, G.; Pelizzi, G. *J. Chem. Soc., Dalton Trans.* **1979**, 96. (b) Filgueiras, C. A. L.; Holand, P. R.; Johnson, B. F. G.; Raitlby, P. R. *Acta Crystallogr. B* **1982**, *B38*, 954. (c) Guo, N.; Lin, Y.-H.; Xi, S.-Q. *Acta Crystallogr. C* **1995**, *C51*, 619. (d) Evans, D. R.; Huang, M.; Segamish, W. M.; Fettingner, J. C.; Williams, T. L. *Inorg. Chem. Commun.* **2003**, *6*, 462.
- (11) (a) Tokunoh, R.; Sodeoka, M.; Aoe, K. I.; Shibasaki, M. *Tetrahedron Lett.* **1985**, *36*, 8035. (b) Pettinari, C.; Pellei, M.; Cavicchio, G.; Crucianelli, M.; Panzeri, W.; Colapietro, M.; Cassetta, A. *Organometallics* **1999**, *18*, 555. (c) Madec, D.; Mingoia, F.; Macovei, C.; Maitro, G.; Giambastiani, G.; Poli, G. *Eur. J. Org. Chem.* **2005**, 552.
- (12) (a) Li, J.-R.; Zhang, R.-H.; Bu, X.-H. *J. Mol. Struct.* **2005**, *737*, 23. (b) Li, J.-R.; Bu, X.-H. *Eur. J. Inorg. Chem.* **2008**, *1*, 27, and references cited herein.
- (13) (a) Zipp, A. P.; Zipp, S. G. *J. Inorg. Nucl. Chem.* **1980**, *42*, 395. (b) Zipp, A. P.; Zipp, S. G. *J. Inorg. Nucl. Chem.* **1981**, *43*, 395. (c) Li, J.-R.; Bu, X.-H.; Zhang, R. H. *Inorg. Chem.* **2004**, *43*, 237. (d) Li, J.-R.; Zhang, R.-H.; Bu, X.-H. *Aust. J. Chem.* **2006**, *59*, 315.
- (14) (a) Khair, N.; Alcludia, F.; Espartero, J.-L.; Rodríguez, L.; Fernandez, I. *J. Am. Chem. Soc.* **2000**, *122*, 7598. (b) Fernandez, I.; Valdivia, V.; Leal, M. P.; Khair, N. *Org. Lett.* **2007**, *9*, 2215.
- (15) In the ^1H -NMR spectra of $[\text{Rh}_2(\text{BTSE})_2\text{Cl}_2]$ **1** dissolved in pyridine-*d*₅ or DMSO-*d*₆, recorded after storing the samples overnight at room temperature, only the typical signal pattern of non-coordinated BTSE was observed.
- (16) Intramolecular hydrogen bonding usually results in a drastic downfield shift of the OH-protons (a) Liu, J.-G.; Ye, B.-H.; Li, H.; Zhen, Q.-X.; Ji, L.-N.; Fu, Y.-H. *J. Inorg. Biochem.* **1999**, *76*, 265, and references cited herein. (b) Várhelyi, C.; Pokol, G.; Gömöry, Á.; Gănescu, A.; Sohár, P.; Liptay, G.; Várhelyi, C. *J. Therm. Anal. Cal.* **2006**, *83*, 701.
- (17) Intramolecular hydrogen bonding also results in a shift of the OH stretch to lower frequencies: Socrates, G. *Infrared and Raman Characteristic Group Frequencies, Tables and Charts, 3rd Ed.*; John Wiley & Sons: Chichester, 2001. See also refs 16a, 16b.

(18) Reference values for OH- and NH-stretches of the employed pyridine derivatives, measured under the same conditions as the complexes (thin film on KBr plates): 3413–3209 cm⁻¹ (s, br, 2-methyl-6-pyridinemethanol), 3412 (s, br, 2-hydroxy-*isopropyl*-pyridine), 3362 and 3285 cm⁻¹ (s, br, 2-aminomethyl-pyridine).

(19) (a) Bryndza, H. E.; Fong, L. K.; Paciello, R. A.; Tam, W.; Bercaw, J. E. *J. Am. Chem. Soc.* **1987**, *109*, 1444. (b) Stoutland, P. O.; Bergman, R. G.; Nolan, S. P.; Hoff, C. D. *Polyhedron* **1988**, *7*, 1429. (c) Bryndza, H. E.; Domaille, P. J.; Tam, W.; Fong, L. K.; Paciello, R. A.; Bercaw, J. E. *Polyhedron* **1988**, *7*, 1441. (d) Holland, P. L.; Andersen, R. A.; Bergman, R. G.; Huang, J.; Nolan, S. P. *J. Am. Chem. Soc.* **1997**, *119*, 12800.

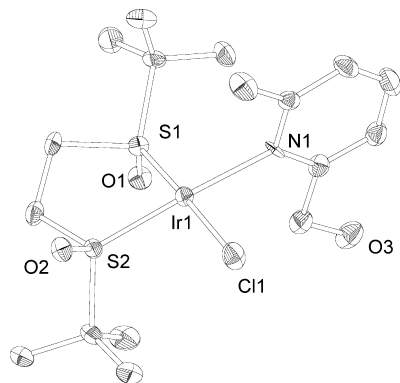
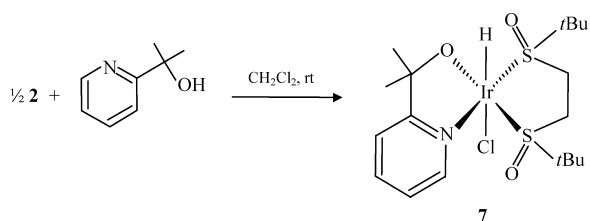


Figure 3. Thermal ellipsoid drawing of [Ir(BTSE)(2-methyl-6-hydroxymethyl-pyridine)(Cl)] **5** at 50% probability; hydrogen atoms are omitted for clarity. Selected bond distances [Å] and angles [deg]: Ir1–Cl1 2.354(2), Ir1–S1 2.181(1), Ir1–S2 2.184(1), Ir1–N1 2.119(3), S1–O1 1.488(3), S2–O2 1.493(3); S1–Ir1–S2 86.36(4), Cl1–Ir1–N1 83.26(9), S1–Ir1–N1 97.76(8), S2–Ir1–Cl1 92.64(4), S1–Ir1–Cl1 177.09(4), S2–Ir1–N1 175.84(9).

Scheme 5



pyridine can be estimated as approximately 17 kJ/mol higher than the CH bond dissociation energy of the methyl group,²⁰ it is likely that the Ir–O bond is stronger than the Ir–C that would have been obtained by C–H activation.

Monitoring the reaction by ¹H NMR spectroscopy, only the signals of the starting materials and the OH activation product **7** were observed after 5 min at room temperature. No signals for an iridium(I) intermediate with a coordinated pyridine-alcohol (analogous to **5**) were observed, implying that the OH bond cleavage takes place as soon as the pyridinic nitrogen coordinates to the iridium center. After 4 h at room temperature, the conversion of **2** to **7** was complete. The ¹H NMR spectrum of **7** exhibits the hydride ligand as a singlet at –20.36 ppm, and the coordinated BTSE gives rise to a typical signal pattern for an asymmetric complex. The IR spectrum exhibits a strong band for the Ir–H stretch at 2204 cm^{–1} and the SO stretches were detected at 1083 and 1123 cm^{–1}, being in the range of S-bonded sulfoxide. No OH signal was observed in the IR spectra of **7**. The activation of OH bonds is an attractive goal, which can lead to the development of new functionalization

(20) To the best of our knowledge, the BDE values of the C–H and O–H bonds of 2-hydroxy-isopropyl-pyridine are not given in literature. According to a recent study, the C–H and O–H BDEs of 2-propanol differ by 18.5 kJ/mol and in the case of *tert*-butanol, they differ by 16.5 kJ/mol. Because these values are very similar for the two different alcohols (within the experimental and calculated errors), we assume that the differences in the O–H and C–H BDEs of the substrate 2-hydroxy-isopropyl-pyridine are also in the same range. Reference (a) Gribov, L. A.; Novakov, I. A.; Pavlyuchko, A. I.; Shumovskii, O. Y. *J. Struct. Chem.* **2007**, *48*, 607.

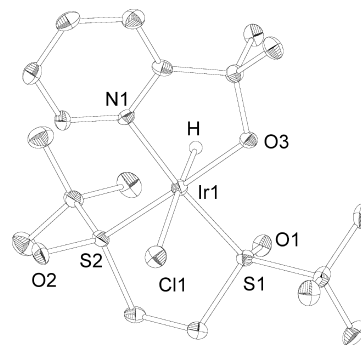


Figure 4. Thermal ellipsoid drawing of [Ir(BTSE)(2-isopropoxy-pyridine)-(H)(Cl)] **7** at 50% probability. Hydrogen atoms are omitted for clarity. Selected bond distances [Å] and angles [deg]: Ir1–H 1.560(59), Ir1–Cl1 2.531(1), Ir1–N1 2.079(2), Ir1–O3 2.032(3), Ir1–S1 2.245(1), Ir1–S2 2.238(1), S1–O1 1.481(3), S2–O2 1.480(3); Cl1–Ir1–H 177.42(216), N1–Ir1–O3 78.01(11), S1–Ir1–S2 85.04(3), H–Ir1–S1 81.15(208), H–Ir1–S2 90.72(219), H–Ir1–N1 96.78(208), Cl1–Ir1–S1 96.28(3), Cl1–Ir1–S2 88.87(3), N1–Ir1–S1 174.60(7), O3–Ir1–S2 177.94(8).

reactions of alcohols or water.^{4–6,21} In our case, the oxidative addition was made possible by the presence of the pyridine directing group and the sterically demanding *isopropylidene* bridge, which helps orient the alcohol function toward the iridium atom and stabilizes the resulting activation product. In case of the **5** and **6**, no cleavage of compounds OH or NH bonds was observed even after prolonged heating or addition of water.

The molecular structure of **7** was confirmed by an X-ray diffraction on crystals grown from a saturated CH₂Cl₂ solution by layering with Et₂O. The iridium atom in **7** is octahedrally coordinated, with the pyridine ring being in plane with the sulfur atoms of BTSE. The hydride and chloride ligands adopt a trans arrangement (Figure 4).

Attempts to cleave the chloride bridges in **1** with the pyridine derivatives, in a similar manner used in case of **2** failed. No reaction took place with 2-hydroxy-*isopropyl*-pyridine, whereas product mixtures were formed with 2-methyl-6-pyridine-methanol and 2-aminomethyl-pyridine. Straightforward reactions were achieved upon abstraction of the chloride ligands with a silver salt in the presence of the bidentate pyridine derivatives, to obtain cationic rhodium complexes.

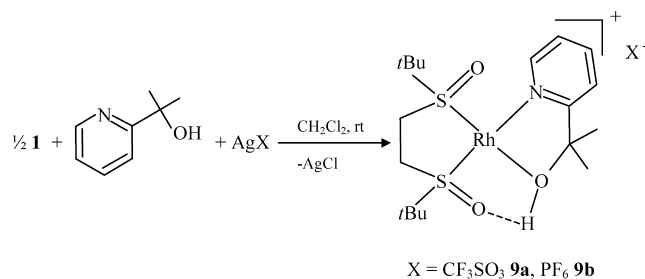
Thus, chloride abstraction from **1** in acetone with AgBF₄ and the addition of one equivalent of 2-aminomethyl-pyridine led to the formation of the cationic Rh-compound [Rh-(BTSE)(2-aminomethyl-pyridine)][BF₄] **8** in good yield as a pale green solid.

The ¹H NMR spectrum of **8** exhibits the NH₂ protons as two broad singlets at 4.74 and 4.93 ppm, which implies that intramolecular hydrogen bonding is not involved. The benzylic protons were detected as two multiplets at 4.45 and 4.65 ppm, due to coordination of the amine-group. The NH

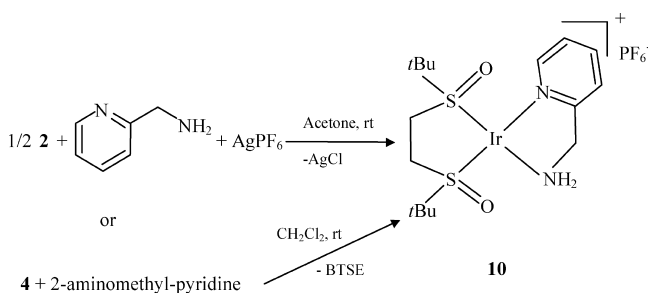
(21) (a) Li, S.; Cui, W.; Wayland, B. B. *Chem. Commun.* **2007**, 4024. (b) Fafard, C. M.; Adhikari, D.; Foxman, B. M.; Mindiola, D. J.; Ozerov, O. V. *J. Am. Chem. Soc.* **2007**, *129*, 10318. (c) Moriya, M.; Takao, T.; Suzuki, H. *Organometallics* **2007**, *26*, 1650.

(22) The SO stretch of the non coordinated meso BMSE was observed at 1016 cm^{–1} when measured as a thin film on KBr plates.

Scheme 6



Scheme 7



stretches appear in the IR spectrum at 3268 and 3328 cm^{-1} , indicating the absence of hydrogen bonding, and the SO-stretch appears at 1063 cm^{-1} for the sulfur-bonded BTSE.

The chloride abstraction approach was also successful in the reaction of **1** with 2-hydroxy-*isopropyl*-pyridine using AgSO_3CF_3 or AgPF_6 , forming complexes $[\text{Rh}(\text{BTSE})(2\text{-hydroxy-}i\text{isopropyl-pyridine})][X]$ ($X = \text{CF}_3\text{SO}_3^- \mathbf{9a}, \text{PF}_6^- \mathbf{9b}$) (Scheme 6).

In contrast to **8**, which did not exhibit hydrogen bonding interaction, the OH group in **9** forms an intramolecular hydrogen bond with the sulfoxide oxygen. This is indicated by the drastic downfield shift of the OH proton in the ^1H NMR spectrum of **9**, which appears as a sharp singlet at 8.58 ppm¹⁶ (in the non-coordinated pyridine alcohol, this signal appears at 5.09 ppm³⁰), and by the OH stretch in the IR spectrum which is shifted to 3166 cm^{-1} .¹⁷ The ^1H - as well the $^{13}\text{C}\{^1\text{H}\}$ NMR spectra of **9a** and **9b** are identical, excluding any interaction with the CF_3SO_3^- or PF_6^- counter-anions. The SO stretches are not really affected by the hydrogen bonding and appear at 1057 and 1078 cm^{-1} . The reaction of **1** with 2-methyl-6-pyridinemethanol in the presence of AgBF_4 , AgPF_6 , or AgSO_3CF_3 was not successful and resulted in complex mixtures that were not further analyzed.

In analogy to the preparation of the rhodium **8**, reaction of the iridium **2** with AgPF_6 and 2-aminomethyl-pyridine resulted in quantitative formation of **10** (Scheme 7).

10 was also formed quantitatively (according to ^1H NMR spectroscopy of the reaction mixture) when the cationic $\text{Ir}(\text{BTSE})_2^+$ **4** was used. The oxygen bonded sulfoxide in **4** is, as expected,^{3–5} relatively labile and was smoothly replaced by the better donor ligand 2-aminomethyl-pyridine. The ^1H NMR spectrum of **10** exhibits the resonances of the NH_2 protons as two broad singlets at 5.71 and 5.91 ppm, giving no evidence for intramolecular hydrogen bonding (also **8**). The NH_2 stretches appear as bands at 3132 and 3226 cm^{-1} .

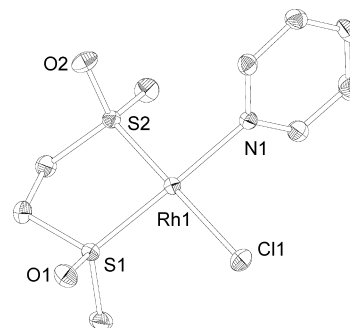


Figure 5. Thermal ellipsoid drawing of $[\text{Rh}(\text{BMSE})(\text{Pyridine})(\text{Cl})] \mathbf{11}$ at 50% probability. Hydrogen atoms are omitted for clarity. Selected bond distances [\AA] and angles [deg]: Rh1–S1 2.179(1), Rh1–S2 2.158(1), Rh1–Cl1 2.367(1), Rh1–N1 2.089(2), S1–O1 1.481(2), S2–O2 1.482(2); S1–Rh1–S2 88.23(2), N1–Rh1–Cl1 89.82(7), S1–Rh1–Cl1 92.32(3), S2–Rh1–N1 89.62(7), S2–Rh1–Cl1 177.70(3), S1–Rh1–N1 177.84(6).

Under forcing conditions, the BTSE ligand can be displaced by the sterically less demanding bis-sulfoxide 1,2-di(methylsulfinyl)ethane (BMSE), which was prepared as the pure *meso* isomer according to a literature procedure.^{26,27} Thus, heating a solution of **1** and BMSE in pyridine at 100 $^\circ\text{C}$ for 20 min led to the formation of $[\text{Rh}(\text{BMSE})(\text{pyridine})(\text{Cl})] \mathbf{11}$.

11 is nearly insoluble in most of the common solvents (MeOH, cold pyridine, H_2O , acetone, benzene, CH_2Cl_2 and it decomposes in CHCl_3 forming a black precipitate) except DMSO. The ^1H NMR spectrum of **11** in $\text{DMSO-}d_6$ at 42 $^\circ\text{C}$ is not very meaningful. The resonances of the BMSE ligand appear as one broad signal at about 3 ppm, and the pyridine protons give rise to three broad singlets. At 93 $^\circ\text{C}$, the ^1H NMR spectrum becomes somewhat more informative. The BMSE ligand gives rise to three broad singlets at 2.98, 3.10, and 3.30 ppm with an integration ratio of 3:3:4 and the pyridine signals appear as two triplets at 7.35 and 7.77 ppm and a broad singlet at 8.60 ppm, in a ratio of 2:1:2. The SO stretches of **11** appear as strong bands at 1067 and 1091 cm^{-1} , which is in the range of S-bonded sulfoxide ligands (the appearance of two bands is a result of the asymmetric nature of **11**).²² **11** partially loses the pyridine ligand during lengthy drying in vacuo, and we were not able to obtain a satisfactory elemental analysis of it. The molecular structure of **11** was obtained by X-ray diffraction of yellow crystals grown at 80 $^\circ\text{C}$ from a concentrated reaction solution. The rhodium atom in **11** is centered in a distorted square plane comprising *meso* BMSE, chloride, and pyridine ligands. Like in the case of **5**, the pyridine ring is orthogonal to the coordination plane of rhodium center (Figure 5).

(23) Recent examples (a) Xu, W.; Lin, J.-L. *Acta Crystallogr.* **2007**, E63, m859. (b) Rubin-Preminger, J. M.; Kozlow, L.; Goldberg, I. *Acta Crystallogr.* **2008**, C64, m83. (c) Pacigová, S.; Gyepes, R.; Tatiarsky, J.; Sivák, M. *Dalton Tran.* **2008**, 121.

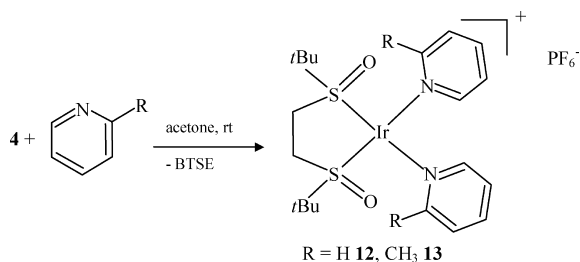
(24) Janiak, C. *J. Chem. Soc., Dalton Trans.* **2000**, 3885, and references therein.

(25) Swart, M.; van der Wijst, T.; Guerra, C. F.; Bickelhaupt, F. M. *J. Mol. Model.* **2007**, 13, 1245, and references therein.

(26) Fehnel, E. A.; Carmack, M. *J. Am. Chem. Soc.* **1949**, 71, 84.

(27) Drabowicz, J.; Łyżwa, P.; Popielarczyk, M.; Mikołajczyk, M. *Synthesis* **1990**, 10, 937.

Scheme 8



Reactivity of the Cationic All-BTSE Rhodium and Iridium Complexes. As described in the synthesis of **10**, the O-bonded BTSE ligand in **4** is labile and can be displaced by 2-aminomethyl-pyridine. It is also possible to displace this ligand by nonchelating donors like pyridine or α -picoline, resulting in formation of the cationic complexes [Ir(BTSE)(pyridine)₂][PF₆] **12** and [Ir(BTSE)(α -picoline)₂][PF₆] **13** (Scheme 8).

13 was isolated in good yield as a yellow solid. The ¹H NMR spectrum of **13** shows a BTSE signal pattern typical for a symmetrical complex (one CH₃ singlet at 1.31 ppm and two multiplets at 2.53 and 3.96 ppm for the CH₂CH₂ backbone), and the picoline ligand gives rise to a set of signals in a correct integration ratio. The SO stretch of the S-bonded sulfoxide appears as a strong band at 1064 cm⁻¹. The analogous pyridine **12** was characterized by NMR spectroscopy and because of the similarity to **12** we didn't isolate this complex. We checked the reactivity of **12** toward water by adding excess water to the reaction mixture in acetone, but even after prolonged heating to 45 °C no reaction took place.

The O-bonded BTSE in the cationic rhodium **3** can be displaced by 1,10-phenanthroline, whereby [Rh(BTSE)(1,10-phenanthroline)][PF₆] **14** was obtained as an orange solid.

The signals of the BTSE protons in **14** as well as the resonances of the 1,10-phenanthroline ligand indicate a symmetrical complex. The UV–vis spectra of the deep-orange-colored complex **14** recorded in CH₂Cl₂ exhibits two intense absorption bands in the UV region at 227 and 270 nm, assigned to ligand centered $\pi \rightarrow \pi^*$ transitions of the 1,10-phenanthroline ligand, and a medium band in the visible region at 374 nm for the $d_{\pi}(\text{Rh}) \rightarrow \pi^*(\text{phenanthroline})$ metal to ligand charge-transfer transitions. The SO stretch at 1078 cm⁻¹ in the IR spectrum implies S-bonding of the BTSE ligand, which was confirmed by an X-ray diffraction study on crystals of **14** obtained by layering a CH₂Cl₂ solution with pentane (Figure 6).

In the solid state, **14** forms dimers by slipped π – π stacking of the 1,10-phenanthroline ligands. This type of crystal packing of 1,10-phenanthroline complexes is known.²³ The observed shortest carbon–carbon contact between the phenanthroline ligands (3.441(7) Å) as well as the centroid–centroid distance of 3.711(9) Å (for the central rings) are consistent with reported experimental²⁴ and calculated²⁵ values for stacked nitrogen-containing aromatic rings.

In summary the neutral as well as cationic complexes [M₂(BTSE)₂Cl₂] (M = Rh **1**, Ir **2**) and [M(BTSE)₂][PF₆] (M = Rh **3**, Ir **4**) are good precursors for the preparation of new

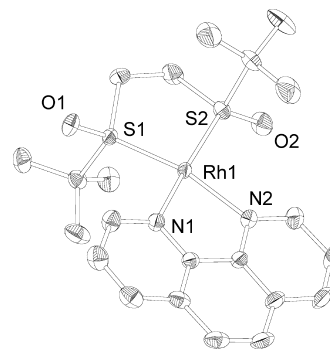


Figure 6. Thermal ellipsoid drawing of the molecular cation of [Rh(BTSE)(1,10-phenanthroline)][PF₆] **14** at 50% probability. Hydrogen atoms are omitted for clarity. Selected bond distances [Å] and angles [deg]: Rh1–S1 2.184(1), Rh1–S2 2.188(10), Rh1–N1 2.099(12), Rh1–N1 2.099(12), S1–O1 1.482(3), S2–O2 1.483(3); S1–Rh1–S2 88.43(3), N1–Rh1–N2 79.12(10), S1–Rh1–N1 96.57(6), S2–Rh1–N2 98.19(8), S1–Rh–N2 165.54(9), S2–Rh1–N1 169.41(7).

sulfoxide-based rhodium and iridium complexes as shown by first studies on the their reactivity toward nitrogen-based donor ligands. So far, intermolecular OH activation reactions of water or aliphatic alcohols with the BTSE compounds, like observed in case of Ir(I) DMSO complexes,^{4,5} was not observed. However, the system is capable of intramolecular oxidative addition of alcohol OH, in preference to C–H activation (formation of **7**). Further work on this topic is in progress.

Experimental Section

General Procedures. All experiments were carried out under an atmosphere of purified nitrogen in a Vacuum Atmospheres glovebox or by standard Schlenk techniques under argon. All solvents were reagent grade or better. All nondeuterated solvents were refluxed over sodium benzophenone ketyl and distilled under an argon atmosphere. Deuterated solvents were used as received. All solvents were degasses with argon and kept over molecular sieves or deteride (in case of acetone) in the glovebox. Commercially available reagents were used as received. Experiments with silver salts were performed protected from light. *t*Bu₂SC₂H₄S/*t*Bu²⁶ and *t*Bu₂SOC₂H₄SO/*t*Bu²⁷ were prepared by modified literature procedures. MeSC₂H₄SMe,²⁸ *meso*-MeSOC₂-H₄SOME (BMSE),²⁹ 2-hydroxy-*iso*-propyl-pyridine,³⁰ [Rh₂(COE)₄-Cl₂],³¹ [Ir₂(COE)₄Cl₂],³² [Rh(COE)₂(O=C(CH₃)₂)] [PF₆]³³ and [Ir(COE)₂(O=C(CH₃)₂)] [PF₆]³⁴ were prepared according to literature procedures. ¹H-, ¹³C-, ¹⁹F-, and ³¹P NMR spectra were recorded on Bruker DPX-250, Bruker DR-400, or Bruker AV-500 spectrometers. ¹³C-, ¹⁹F-, and ³¹P NMR are broadband ¹H decoupled. NMR chemical shifts are reported in ppm downfield from tetram-

(28) Alekminskaya, O. V.; Russavskaya, N. V.; Korchevin, N. A.; Deryagina, E. N. *Russ. J. Gen. Chem.* **2002**, *1*, 75.

(29) Hull, C. M.; Bargar, T. W. *J. Org. Chem.* **1975**, *40*, 3152.

(30) Tsukahara, T.; Swenson, D. C.; Jordan, R. F. *Organometallics* **1997**, *16*, 3303.

(31) Hofmann, P.; Meier, C.; Englert, U.; Schmidt, U. *Chem. Ber.* **1992**, *125*, 353.

(32) Van der Ent, A.; Onderlinden, A. L. *Inorg. Synth.* **1990**, *28*, 90.

(33) Windmüller, B.; Nürnberg, O.; Wolf, J.; Werner, H. *Eur. J. Inorg. Chem.* **1999**, 613.

(34) Dorta, R.; Goikhmann, R.; Milstein, D. *Organometallics* **2003**, *22*, 2806.

(35) (a) Sheldrick, G. M. *SHELXS-97, Programm for Crystal Structure Solution*; University of Göttingen, Göttingen, Germany, 1997. (b) Sheldrick, G. M. *SHELXL-97, Program for Crystal Structure Refinement*; University of Göttingen, Göttingen, Germany, 1997.

Table 1. X-ray Data Collection and Processing Parameters

	1	2	3	5	7	11	14
formula	C ₂₀ H ₄₄ Cl ₂ O ₄ Rh ₂ S ₄	C ₂₀ H ₄₄ S ₄ O ₄ Cl ₂ Ir ₂	C ₂₀ H ₄₄ O ₄ S ₄ Rh* PF ₆ *C ₃ H ₆ O	C ₁₇ H ₃₁ NO ₃ ClS ₂ Ir	C ₁₈ H ₃₃ NO ₃ ClS ₂ Ir	C ₉ H ₁₅ ClO ₂ RhS ₂	C ₂₂ H ₃₀ N ₂ O ₂ RhS ₂ * PF ₆ *1/2CH ₂ Cl ₂
fw	753.55	932.09	782.79	589.20	603.22	371.70	708.94
cryst. syst.	hexagonal	hexagonal	orthorhombic	monoclinic	orthorhombic	monoclinic	monoclinic
space group	<i>P</i> 6 ₅	<i>P</i> 6 ₅	<i>Pbcn</i>	<i>P</i> 2 ₁ / <i>c</i>	<i>P</i> 2 ₁ 2 ₁ 2 ₁	<i>P</i> 2 ₁ / <i>c</i>	<i>P</i> 2 ₁ / <i>c</i>
<i>a</i> /Å	21.5055(5)	21.6261(8)	12.6747(2)	13.9210(2)	9.8091(2)	8.1388(1)	13.6477(10)
<i>b</i> /Å	21.5055(5)	21.6261(8)	22.5346(3)	10.4556(2)	11.2920(1)	17.7196(3)	10.7513(6)
<i>c</i> /Å	11.7732(2)	11.7931(15)	24.0876(4)	14.9360(2)	20.0011(4)	9.7850(1)	20.2994(16)
β /deg				105.9672(11)		108.4816(10)	109.557(9)
<i>V</i> /Å ³	4715.6(2)	4776.6(6)	6879.9(2)	2090.1(1)	2215.4(1)	1338.38	2806.7(3)
<i>Z</i>	6	6	8	4	4	4	2
μ /mm ⁻¹	1.508	8.802	0.848	6.732	6.353	1.772	0.974
no. indep reflns.	6415	3097	9478	7628	4717	3183	4505
no. of observed reflns ^a	33 860	37 326	60 953	47 992	18 603	20 276	25 593
no. of params	302	289	355	234	248	147	333
GOF	1.200	1.187	1.137	1.028	1.036	1.106	1.040
Final R ^b , wR ^c	0.0361; 0.0394	0.0208; 0.0230	0.0702; 0.0818	0.0341; 0.0554	0.0232; 0.0270	0.0308; 0.0345	0.0359; 0.0412

^a Reflections with $I > 2\sigma(I)$. ^b $R = \sum |F_o| - |F_c| / \sum |F_o|$. ^c $wR2 = \{\sum [w(F_o^2 - F_c^2)^2] / \sum [w(F_o^2)^2]\}^{1/2}$.

ethylsilane (¹H, ¹³C), CCl₃F (¹⁹F), or H₃PO₄ (³¹P) and the residual solvent peak as the reference. Abbreviations used in the NMR data are as follows: s, singlet; d, doublet; dd, doublet of doublets; t, triplet; td, triplet of doublets; sept, septet; m, multiplet. Other abbreviations: room temperature = rt. Assignments of the ¹³C{¹H} NMR signals were confirmed by ¹³C DEPT measurements. FTIR spectra were recorded on a Nicolet PROTEGE 460 spectrometer as thin films on KBr plates. The IR values are given in [cm⁻¹]. Elemental analyses were performed by H. Kolbe, Mikroanalytisches Laboratorium, Mühlheim, Germany.

***t*Bu₂SC₂H₄SrBu.** A mixture of KOH (12.3 g, 0.22 mol), ethanol (100 mL), and 2-methyl-2-propanethiol (24.8 mL, 0.22 mol) was heated under reflux for 30 min. After cooling to 60 °C, 1,2-dibromoethane (20.5 g, 0.11 mol) was added dropwise over a period of 30 min, during which a white precipitate (KBr) was formed and the reaction mixture started to reflux without external heating. After the addition, the mixture was heated under reflux for 30 min and then cooled down to room temperature by means of a waterbath. All volatiles were removed in vacuo, and 200 mL of water were added to the residue. The organic layer was separated and dried over MgSO₄. After removing of all volatiles in vacuo, the pure bis-sulfide was obtained as a slightly yellow liquid. Yield: 14.9 g (72.2 mmol; 66%). ¹H NMR (250 MHz, 25 °C, CDCl₃): 1.17 (C(CH₃)₃), 2.55 (CH₂CH₂). ¹³C{¹H}-NMR (63 MHz, 25 °C, CDCl₃): 28.8 (CH₂CH₂), 30.9 (C(CH₃)₃), 42.3 (C(CH₃)₃).

***t*Bu₂SOC₂H₄SO/*t*Bu (BTSE).** *t*BuSC₂H₄SrBu (4.9 g, 23.8 mmol) and H₂O₂ (12.4 g, 109.8 mmol, 30% in H₂O) were dissolved in 110 mL methanol. A solution of H₂SO₄ (0.35 g, 3.57 mmol) in 9.5 mL 2-propanol was added, and the reaction mixture was stirred at room temperature for 5 h. 200 mL water was added and the solution was saturated with NaCl. The product was extracted with 3 × 100 mL CHCl₃. The combined organic phases were dried over MgSO₄ and all volatiles were removed in vacuo. The crude product was recrystallized from a hot hexane/ethylacetate (1:1) solution by cooling to -30 °C to yield 4.5 g (79.3%) of a white, crystalline solid as a mixture of the *RR/SS*-pair and the *meso*-isomer (83% *RS*, 17% *meso*). Sulfones were not detected. Analytical data was consistent with the given literature data.^{9b}

[Rh₂(BTSE)₂Cl₂] (1). [Rh₂(COE)₄Cl₂] (300 mg, 0.42 mmol) and BTSE (400 mg, 1.68 mmol) were dissolved in 5 mL CH₂Cl₂ and stirred at room temperature for 2 h, resulting in an deep orange solution. Thirty mL of pentane were added and an orange precipitate was formed. The precipitate was filtered off and washed with 2 × 10 mL pentane. The product was dried in vacuo to yield 273 mg (86.9%) of an orange powder. Crystals suitable

for X-ray diffraction were obtained by layering a CH₂Cl₂-solution with pentane. Elemental analysis: Calcd (%) for C₂₀H₄₄S₄O₄Cl₂Rh₂ (753.55 g/mol): C 31.88, H 5.89; found: C 31.50, H 6.25. IR: 681 (m), 1072 (vs, ν_{SO}), 1106 (s), 1166 (m), 1362 (m), 1387 (m), 1472 (m), 2859 (m), 2927 (s), 2970 (s). ¹H NMR (500 MHz, 25 °C, CD₂Cl₂): 1.61 (s, 18 H, C(CH₃)₃), 2.79 (m, 2 H, CH₂CH₂), 3.21 (m, 2 H, CH₂CH₂). ¹³C{¹H}-NMR (126 MHz, 25 °C, CD₂Cl₂): 24.3 (C(CH₃)₃), 49.9 (d, ²J_{RhC} = 4.2 Hz, CH₂CH₂), 65.4 (d, ²J_{RhC} = 2.5 Hz, C(CH₃)₃).

[Ir₂(BTSE)₂Cl₂] (2). [Ir₂(COE)₄Cl₂] (400 mg, 0.45 mmol) and BTSE (480 mg, 1.55 mmol) were dissolved in 30 mL CH₂Cl₂ and stirred at room temperature for 5 h. The orange solution was concentrated in vacuo to about 7 mL. Et₂O (80 mL) was added forming a yellow precipitate. The precipitate was filtered off, washed with 2 × 15 mL Et₂O, and the product was dried in vacuo to yield 225 mg (46.8%) of a yellow powder. Crystals suitable for X-ray diffraction were obtained by slow diffusion of pentane in a CH₂Cl₂-solution. Elemental analysis Calcd. (%) for C₂₀H₄₄S₄O₄Cl₂Ir₂ (932.18 g/mol): C 25.77, H 4.76; found: C 25.97, H 4.71. IR: 689 (m), 732 (w), 817 (w), 919 (w), 1072 (vs, ν_{SO}), 1106 (s), 1174 (m), 1362 (m), 1396 (m), 1472 (m), 2868 (w), 2936 (m), 2970 (m). ¹H NMR (500 MHz, 25 °C, CD₂Cl₂): 1.56 (s, 18 H, C(CH₃)₃), 2.51 (m, 2 H, CH₂CH₂), 3.25 (m, 2 H, CH₂CH₂). ¹³C{¹H}-NMR (126 MHz, 25 °C, CD₂Cl₂): 24.4 (C(CH₃)₃), 52.5 (CH₂CH₂), 65.3 (C(CH₃)₃).

[Rh(BTSE)₂][PF₆] (3). [Rh(COE)₂(O=C(CH₃)₂)]PF₆ (200 mg, 0.34 mmol) and BTSE (260 mg, 1.09 mmol) were dissolved in 4 mL CH₂Cl₂ and the reaction mixture was stirred at room temperature for 1 h. Upon addition of 20 mL pentane, a yellow precipitate was formed, which was filtered off and washed with 2 × 15 mL Et₂O. The product was dried in vacuo to yield 240 mg (97.4%) of a yellow powder. Crystals suitable for X-ray diffraction were obtained by slow diffusion of Et₂O in a acetone-solution. Elemental analysis: Calcd. (%) for C₂₀H₄₄S₄O₄PF₆Rh (724.71 g/mol): C 33.15, H 6.12; found: C 33.06, H 6.18. ESI/MS *m/z* (%): 579.78 (100) [Rh(BTSE)₂]⁺, 145.11 (100) [PF₆]⁻. IR: 843 (vs, ν_{P-F}), 936 (m, ν_{SO}), 1072 (s, ν_{SO}), 1106 (m), 1174 (w), 1387 (m), 1472 (m), 2868 (w), 2936 (m), 2970 (m). ¹H NMR (500 MHz, 25 °C, CD₂Cl₂): 1.40 (s, 18 H, C(CH₃)₃), 1.59 (s, 18 H, C(CH₃)₃), 2.50 (m, 2 H, CH₂CH₂), 3.02 (s, 2 H, CH₂CH₂), 3.30 (s, 2 H, CH₂CH₂), 3.41 (s, 2 H, CH₂CH₂). ¹³C{¹H}-NMR (126 MHz, 25 °C, CD₂Cl₂): 22.89 (C(CH₃)₃), 23.95 (C(CH₃)₃), 42.16 (CH₂CH₂), 50.6 (d, ²J_{RhC} = 4.7 Hz, CH₂CH₂), 56.8 (C(CH₃)₃), 65.3 (d, ²J_{RhC} = 2.5 Hz, C(CH₃)₃). ³¹P{¹H}-NMR (202 MHz, 25 °C, CD₂Cl₂): -144.3 (sept, 1 P, ¹J_{FP} = 712.1 Hz, PF₆).

[Ir(BTSE)₂][PF₆] (**4**). [Ir(COE)₂(O=C(CH₃)₂)] [PF₆] (550 mg, 0.82 mmol) and BTSE (720 mg, 3.03 mmol) were dissolved in 12 mL CH₂Cl₂, and the reaction mixture was stirred at room temperature 3 h. Pentane (40 mL) was added to the reaction solution and a yellow precipitate was formed, which was filtered off, washed with 15 mL pentane, 15 mL Et₂O, and dried in vacuo to yield 534 mg (73.5%) of a yellow powder. Elemental analysis: Calcd. (%) for C₂₀H₄₄S₄O₄PF₆Ir (814.02 g/mol): C 29.51, H 5.45; found: C 29.47, H 5.40. ESI/MS *m/z* (%): 669.91 (100) [Ir(BTSE)₂]⁺, 145.11 (100) [PF₆]⁻. IR: 843 (vs, ν_{P–F}), 919 (m, ν_{SO}), 1081 (m, ν_{SO}), 1115 (w), 1165 (w), 1387 (m), 1421 (m), 1472 (m), 2877 (w), 2936 (m), 2970 (m). ¹H NMR (250 MHz, 25 °C, CD₂Cl₂): 1.45 (s, 18 H, *t*Bu-CH₃), 1.51 (s, 18 H, *t*Bu-CH₃), 2.23 (m, 2 H, SCH₂), 3.12 (m, 2 H, SCH₂), 3.34 (m, 4 H, SCH₂). ¹³C{¹H}-NMR (126 MHz, 25 °C, CD₂Cl₂): 22.9 (*t*Bu-CH₃), 23.9 (*t*Bu-CH₃), 42.1 (SCH₂), 54.1 (SCH₂), 57.4 (*t*Bu-C), 65.5 (*t*Bu-C). ³¹P{¹H}-NMR (202 MHz, 25 °C, CD₂Cl₂): -144.3 (sept, 1 P, ¹J_{FP} = 710.1 Hz, PF₆⁻).

[Ir(BTSE)(2-methyl-6-pyridinemethanol)(Cl)] (**5**). A solution of 2-methyl-6-pyridinemethanol (26.3 mg, 0.22 mmol) in 5 mL CH₂Cl₂ was added to solid [Ir₂(BTSE)₂Cl₂] **2** (100 mg, 0.11 mmol) and the yellow solution was stirred for 2 h. All volatiles were removed in vacuo, the residue washed with 10 mL Et₂O, and the yellow product was dried in vacuo. Yield: 115 mg (92.2%). Crystals suitable for X-ray diffraction were grown by layering a saturated CH₂Cl₂ solution with pentane. Elemental analysis: Calcd. (%) for C₁₇H₃₁S₂O₃NClIr (589.24 g/mol): C 34.65, H 5.30, N 2.38; found: C 34.54, H 5.45, N 2.32. ESI/MS *m/z* (%): 554.69 (100) [M-Cl]⁺. IR: 689 (m), 723 (w), 791 (w), 1064 (vs, ν_{SO}), 1107 (m), 1174 (m), 1370 (m), 1464 (s), 1566 (w), 1609 (m), 2860 (w), 2928 (m), 2963 (m), 3047 (w), 3387 (s, br, ν_{OH}). ¹H NMR (500 MHz, 25 °C, CD₂Cl₂): δ = 1.25 (s, 9 H, C(CH₃)₃), 1.74 (s, 9 H, C(CH₃)₃), 2.84 (m, 2 H, CH₂CH₂), 3.14 (m, 2 H, CH₂CH₂), 3.29 (s, 3 H, aryl-CH₃), 4.75 (d, 1 H, ²J_{HH} = 12.7 Hz, aryl-CH₂), 5.16 (s, br, 1 H, OH), 6.31 (d, 2 H, ²J_{HH} = 12.7 Hz, aryl-CH₂), 7.31 (d, 1 H, ³J_{HH} = 7.6 Hz, aryl-H₅), 7.49 (d, 1 H, ³J_{HH} = 7.7 Hz, aryl-H₃), 7.80 (t, 1 H, ³J_{HH} = 7.7 Hz, aryl-H₄). ¹³C{¹H}-NMR (126 MHz, 25 °C, CD₂Cl₂): δ = 23.23 (C(CH₃)₃), 24.65 (C(CH₃)₃), 29.29 (aryl-CH₃), 50.07 (CH₂CH₂), 52.03 (CH₂CH₂), 63.60 (C(CH₃)₃), 65.13 (C(CH₃)₃), 66.66 (aryl-CH₂), 123.96 (aryl-C₅), 125.40 (aryl-C₃), 138.75 (aryl-C₄), 160.62 (aryl-C₆), 163.82 (aryl-C₂).

[Ir(BTSE)(2-aminomethyl-pyridine)(Cl)] (**6**). [Ir₂(BTSE)₂Cl₂] **2** (15.8 mg, 0.017 mmol) and 2-aminomethyl-pyridine (3.7 mg, 0.034 mmol) were dissolved in 1 mL CH₂Cl₂ and kept overnight at room temperature. The green solution was layered with 3 mL Et₂O, and a light green precipitate was formed. The product was filtered off, washed with 3 mL Et₂O and dried in vacuo to yield 16.1 mg (82.5%) of a light green powder. Elemental analysis: Calcd. (%) for C₁₆H₃₀S₂O₂N₂ClIr (574.23 g/mol): C 33.47, H 5.27, N 4.88; found: C 33.26, H 5.35, N 5.02. ESI/MS *m/z* (%): 539.54 (100) [M-Cl]⁺. IR: 698 (m), 766 (w), 853 (w), 1055 (vs, ν_{SO}), 1070 (vs, ν_{SO}), 1166 (m), 1362 (m), 1472 (m), 1609 (w), 2919 (s), 2979 (s), 3217 (m, br, ν_{NH}). ¹H NMR (500 MHz, 25 °C, CD₂Cl₂): 1.41 (s, 9 H, C(CH₃)₃), 1.59 (s, 9 H, C(CH₃)₃), 2.29 (m, 2 H, CH₂CH₂), 3.62 (m, 1 H, CH₂CH₂), 3.86 (m, 1 H, CH₂CH₂), 4.29 (d, 1 H, ²J_{HH} = 13.5 Hz, aryl-CH₂), 4.90 (s, br, 1 H, NH₂), 4.95 (d, 1 H, ²J_{HH} = 15.2 Hz), 7.42 (t, 1 H, ³J_{HH} = 6.6 Hz, aryl-H₅), 7.77 (d, 1 H, ³J_{HH} = 7.8 Hz, aryl-H₃), 8.00 (td, 1 H, ³J_{HH} = 7.8 Hz, ⁴J_{HH} = 1.5 Hz, aryl-H₄), 8.24 (s, br, 1 H, NH₂), 9.36 (d, 1 H, ³J_{HH} = 5.1 Hz, aryl-H₆). ¹³C{¹H}-NMR (126 MHz, 25 °C, CD₂Cl₂): = 23.96 (C(CH₃)₃), 24.02 (C(CH₃)₃), 51.86 (CH₂CH₂), 52.86 (CH₂CH₂), 55.23 (aryl-CH₂), 65.52 (C(CH₃)₃), 65.55 (C(CH₃)₃), 122.37 (aryl-C₅), 123.60 (aryl-C₃), 139.64 (aryl-C₄), 152.53 (aryl-C₆), 164.19 (aryl-C₂).

[Ir(BTSE)(2-isopropoxy-pyridine)(H)(Cl)] (**7**). [Ir₂(BTSE)₂Cl₂] **2** (15.8 mg, 0.017 mmol) and 2-hydroxy-isopropyl-pyridine (4.6 mg, 0.034 mmol) were dissolved in 1 mL CH₂Cl₂ and kept overnight at room temperature. The yellow solution was layered with 3 mL Et₂O and a yellow precipitate was formed. The product was filtered off, washed with 3 mL Et₂O, and dried in vacuo to yield 17.3 mg (84.3%) of a bright yellow powder. Crystals suitable for X-ray diffraction were grown by layering a CH₂Cl₂-solution with Et₂O. Elemental analysis: Calcd. (%) for C₁₈H₃₃S₂O₃NClIr (603.27 g/mol): C 35.84, H 5.51, N 2.32; found: C 35.32, H 5.40, N 2.56. ESI/MS *m/z* (%): 568.59 (100) [M-Cl]⁺. IR: 783 (w), 987 (w), 1021 (w), 1060 (w), 1083 (vs, ν_{SO}), 1123 (vs, ν_{SO}), 1174 (s), 1370 (m), 1472 (m), 1609 (m), 2204 (s, ν_{NH}), 2928 (l), 2970 (s). ¹H NMR (400 MHz, 25 °C, CD₂Cl₂): δ = -20.36 (s, 1 H, Ir-H), 1.40 (s, 9 H, C(CH₃)₃), 1.45 (s, 3 H, C(CH₃)₂), 1.62 (s, 3 H, C(CH₃)₂), 3.13 (m, 1 H, CH₂CH₂), 3.27 (m, 1 H, CH₂CH₂), 3.82 (m, 1 H, CH₂CH₂), 4.52 (m, 1 H, CH₂CH₂), 7.24 (m, 2 H, aryl-H₃₊₅), 7.86 (td, 1 H, ³J_{HH} = 7.7 Hz, ⁴J_{HH} = 1.5 Hz, aryl-H₄), 9.01 (dd, 1 H, ³J_{HH} = 6.3 Hz, ⁴J_{HH} = 1.5 Hz, aryl-H₆). ¹³C{¹H}-NMR (101 MHz, 25 °C, CD₂Cl₂): δ = 23.43 (C(CH₃)₃), 24.64 (C(CH₃)₃), 29.28 (C(CH₃)₂), 31.74 (C(CH₃)₂), 50.81 (CH₂CH₂), 51.45 (CH₂CH₂), 66.81 (C(CH₃)₃), 67.32 (C(CH₃)₃), 84.86 (aryl-C(CH₃)₂), 120.78 (aryl-C₅), 123.07 (aryl-C₃), 138.36 (aryl-C₄), 151.49 (aryl-C₆), 176.66 (aryl-C₂).

[Rh(BTSE)(2-aminomethyl-pyridine)] [BF₄] (**8**). [Rh₂(BTSE)₂-Cl₂] **1** (50.0 mg, 0.067 mmol) and 2-aminomethyl-pyridine (14.4 mg, 0.133 mmol) were dissolved in 5 mL acetone and stirred at room temperature for 10 min. AgBF₄ (25.9 mg, 0.133 mmol) dissolved in 2 mL acetone was added and the reaction mixture was stirred for 15 min. The formed precipitate was removed by filtration over cotton/celite, and all volatiles of the green filtrate were removed in vacuo. The residue was washed with 10 mL Et₂O and 10 mL pentane. The product was dried in vacuo to yield 60 mg (73.6%) of a pale-green powder. Elemental analysis: Calcd. (%) for C₁₆H₃₀N₂S₂O₂RhBF₄ (536.27 g/mol): C 35.84, H 5.64, N 5.22; found: C 35.96, H 5.70, N 5.30. ESI/MS *m/z* (%): 449.58 (100) [Rh(BTSE)(2-aminomethyl-pyridine)]⁺, 87.17 (100) [BF₄]⁻. IR: 681 (m), 732 (w), 826 (w), 1047 (vs, ν_{BF}), 1063 (vs, ν_{SO}), 1166 (m); 1362 (w), 1472 (m), 1608 (m), 2877 (w), 2953 (m), 2970 (m), 3157 (w), 3268 (m, ν_{NH}), 3328 (m, ν_{NH}). ¹H NMR (400 MHz, 17 °C, acetone-*d*₆): = 1.50 (s, 9 H, C(CH₃)₃), 1.59 (s, 9 H, C(CH₃)₃), 2.52 (m, 2 H, CH₂CH₂), 4.11 (m, 2 H, CH₂CH₂), 4.45 (m, 1 H, aryl-CH₂), 4.65 (m, 1 H, aryl-CH₂), 4.74 (s, br, 1 H, NH₂), 4.93 (s, br, 1 H, NH₂), 7.61 (t, 1 H, ³J_{HH} = 6.7 Hz, aryl-H₅), 7.79 (d, 1 H, ³J_{HH} = 7.9 Hz, aryl-H₃), 8.13 (dt, 1 H, ³J_{HH} = 7.8 Hz, ⁴J_{HH} = 1.5 Hz, aryl-H₄), 9.09 (d, 1 H, ³J_{HH} = 5.6 Hz, aryl-H₂). ¹³C{¹H}-NMR (101 MHz, 25 °C, acetone-*d*₆): = 23.36 (C(CH₃)₃), 23.81 (C(CH₃)₃), 51.04 (d, ²J_{RhC} = 2.6 Hz, CH₂CH₂), 51.34 (aryl-CH₂), 52.83 (CH₂CH₂), 64.99 (C(CH₃)₃), 65.54 (d, ²J_{RhC} = 2.6 Hz, C(CH₃)₃), 122.63 (aryl-C₅), 123.90 (aryl-C₃), 140.19 (aryl-C₄), 152.03 (aryl-C₆), 164.03 (aryl-C₂).

[Rh(BTSE)(2-hydroxy-isopropyl-pyridine)] [9] (**X** = CF₃SO₃, **9a**, PF₆ **9b**). **9a**: [Rh₂(BTSE)₂Cl₂] **1** (20.0 mg, 0.027 mmol) and 2-hydroxy-isopropyl-pyridine (7.3 mg, 0.053 mmol) were dissolved in 1 mL CH₂Cl₂ and stirred at room temperature for 10 min. A solution of AgSO₃CF₃ (13.6 mg, 0.053 mmol) in 3 mL CH₂Cl₂ was then added, and the reaction mixture was stirred for 90 min. The formed precipitate was removed by filtration over cotton/celite, and all volatiles of the orange filtrate were removed in vacuo. The residue was washed with 10 mL Et₂O and dried in vacuo to yield 26 mg (81.7%) of an orange powder. **9b**: [Rh₂(BTSE)₂Cl₂] **2** (20.0 mg, 0.027 mmol) and 2-hydroxy-isopropyl-pyridine (7.3 mg, 0.053 mmol) were dissolved in 2 mL acetone and stirred at room

temperature for 10 min. A solution of AgPF₆ (13.4 mg, 0.053 mmol) in 3 mL acetone was then added, and the reaction mixture was stirred for 20 min. The formed precipitate was removed by filtration over cotton/celite and all volatiles of the yellow filtrate were removed in vacuo. The residue was washed with 10 mL Et₂O and dried in vacuo to yield 33 mg (93.8%) of an orange powder. Elemental analysis (**9a**): Calcd. (%) for C₁₉H₃₃S₃O₆F₃NRh (627.58 g/mol): C 36.36, H 5.30, N 2.23; found: C 36.49, H 5.36, N 2.28. ESI/MS *m/z* (%): **9a**: 478.31 (100) [Rh(BTSE)(2-hydroxy-isopropyl-pyridine)]⁺, 148.88 (100) [CF₃SO₃]⁻. **9b**: 478.37 (100) [Rh-(BTSE)(2-hydroxy-isopropyl-pyridine)]⁺, 144.93 (100) [PF₆]⁻. IR: **9a**: 640 (s), 696 (w, CF₃SO₃), 787 (w), 1028 (s, CF₃SO₃), 1057 (s, ν_{SO}), 1077 (s, ν_{SO}), 1157 (s, CF₃SO₃), 1243 (vs, CF₃SO₃), 1276 (vs, CF₃SO₃), 1370 (m), 1472 (w), 2970 (s), 3150 (m, br, ν_{OH}). **9b**: 689 ((w), 843 (vs, ν_{PF}), 1057 (s, ν_{SO}), 1078 (s, ν_{SO}), 1166 (m), 1243 (m), 1464 (m), 2970 (s), 3166 (m, br, ν_{OH}). ¹H NMR (400 MHz, 25 °C, acetone-*d*₆): **9a**, **9b**: 1.56 (s, 9 H, C(CH₃)₃), 1.64 (s, 9 H, C(CH₃)₃), 1.95 (s, 3 H, C(CH₃)₂), 2.07 (s, 3 H, C(CH₃)₂), 2.66 (m, 2 H, CH₂CH₂), 3.98 (m, 1 H, CH₂CH₂), 4.18 (m, 1 H, CH₂CH₂), 7.68 (m, 1 H, aryl-*H*₅), 7.81 (d, 1 H, ³J_{HH} = 7.9 Hz, aryl-*H*₃), 8.22 (td, 1 H, ³J_{HH} = 7.8 Hz, ⁴J_{HH} = 1.6 Hz, aryl-*H*₄), 8.58 (s, 1 H, OH), 9.19 (d, 1 H, ³J_{HH} = 5.58 Hz, aryl-*H*₆). ¹³C{¹H}-NMR (101 MHz, 25 °C, acetone-*d*₆): **9a**, **9b**: 22.96 (C(CH₃)₃), 23.51 (C(CH₃)₃), 27.36 (C(CH₃)₂), 31.85 (C(CH₃)₂), 50.09 (d, ²J_{RhC} = 3.5 Hz, CH₂CH₂), 53.64 (d, ²J_{RhC} = 3.3 Hz, CH₂CH₂), 64.90 (C(CH₃)₃), 66.58 (d, ²J_{RhC} = 2.8 Hz, C(CH₃)₃), 84.22 (C(CH₃)₂), 121.75 (aryl-*C*₅), 124.28 (aryl-*C*₃), 140.50 (aryl-*C*₄), 151.40 (aryl-*C*₆), 166.12 (aryl-*C*₂). ¹⁹F{¹H}-NMR (376 MHz, 25 °C, acetone-*d*₆): **9a**: -78.95 (s, 3 F, CF₃SO₃). ³¹P{¹H}-NMR (101 MHz, 25 °C, acetone-*d*₆): **9b**: -143.67 (sept, 1 P, ¹J_{FP} = 707.8 Hz, PF₆).

[Ir(BTSE)(2-aminomethyl-pyridine)][PF₆] (10): Method 1. [Ir₂(BTSE)₂Cl₂] **2** (15.8 mg, 0.017 mmol) and 2-aminomethylpyridine (3.7 mg, 0.034 mmol) were dissolved in 3 mL acetone and stirred at room temperature for 10 min. A solution of AgPF₆ (8.6 mg, 0.034 mmol) in 2 mL acetone was added dropwise and the reaction mixture was stirred for 1 h at room temperature. The precipitate was removed by filtration over cotton/celite and all volatiles were removed from the yellow filtrate to yield 20.7 mg (88.9%) of a yellow powder. **Method 2.** [Ir(BTSE)₂][PF₆] **4** (20.0 mg, 0.025 mmol) and 2-aminomethylpyridine (2.7 mg, 0.025 mmol) were dissolved in 1 mL CH₂Cl₂ and kept overnight at room temperature. The Reaction solution was layered with 3 mL Et₂O and a yellow solid was formed. The solid was filtered off, washed with 2 × 3 mL Et₂O and dried *in vacuo* to yield 9.0 mg (52.7%) of a yellow powder. Elemental analysis: Calcd. (%) for C₁₆H₃₀S₂O₂N₂IrPF₆ (683.74 g/mol): C 28.11, H 4.42, N 4.10; found: C 27.96, H 4.37, N 3.96. ESI/MS *m/z* (%): 539.61 (100) [Ir(BTSE)(2-aminomethyl-pyridine)]⁺, 145.05 (100) [PF₆]⁻. IR: 698 (w), 843 (vs, ν_{PF}), 1056 (s, ν_{SO}), 1070 (s, ν_{SO}), 1106 (m), 1166 (m), 1242 (w), 1362 (w), 1472 (m), 1617 (m), 2877 (w), 2928 (m), 2970 (m), 3132 (m, ν_{NH}), 3226 (m, ν_{NH}). ¹H NMR(400 MHz, 25 °C, acetone-*d*₆): 1.40 (s, 9 H, C(CH₃)₃), 1.52 (s, 9 H, C(CH₃)₃), 2.32 (m, 2 H, CH₂CH₂), 3.90 (m, 1 H, CH₂CH₂), 4.14 (m, 1 H, CH₂CH₂), 4.58 (d, 1 H, ²J_{HH} = 2.8 Hz, aryl-*CH*₂), 4.61 (d, 1 H, ²J_{HH} = 2.8 Hz, aryl-*CH*₂), 5.71 (s, br, 1 H, NH₂), 5.91 (s, br, 1 H, NH₂), 7.62 (t, 1 H, ³J_{HH} = 7.2 Hz, aryl-*H*₅), 7.88 (d, 1 H, ³J_{HH} = 7.9 Hz, aryl-*H*₃), 8.19 (td, 1 H, ³J_{HH} = 7.7 Hz, ⁴J_{HH} = 1.5 Hz, aryl-*H*₄), 9.40 (d, 1 H, ³J_{HH} = 5.7 Hz, aryl-*H*₆). ¹³C{¹H}-NMR (101 MHz, 25 °C, acetone-*d*₆): 23.28 (C(CH₃)₃), 23.62 (C(CH₃)₃), 51.99 (CH₂CH₂), 53.40 (CH₂CH₂), 56.11 (aryl-*CH*₂), 65.30 (C(CH₃)₃), 65.74 (C(CH₃)₃), 122.73 (aryl-*C*₅), 124.39 (aryl-*C*₃), 140.56 (aryl-*C*₄), 152.80 (aryl-*C*₆), 164.48 (aryl-*C*₂). ³¹P{¹H}-NMR (162 MHz, 25 °C, acetone-*d*₆): -142.14 (sept, 1 P, ¹J_{FP} = 707.6 Hz, PF₆).

[Rh(BMSE)(pyridine)(Cl)] (11). [Rh₂(BTSE)₂Cl₂] **1** (60 mg, 0.080 mmol) and *meso*-BMSE (24.6 mg, 0.159 mmol) were dissolved in 5 mL pyridine and heated to 100 °C for 20 min, forming a deep-orange solution and a black precipitate. The solution was filtered hot over cotton to remove small amounts of elemental rhodium and after cooling to room temperature, 20 mL Et₂O was added, forming a light-yellow precipitate. The precipitate was filtered off, washed with 15 mL Et₂O, and dried in vacuo for 20 min to yield 42 mg (71.1%) of a light-yellow powder. Crystals suitable for X-ray diffraction were obtained by heating a mixture of [Rh₂(BTSE)₄(Cl)₂] (20 mg, 0.027 mmol) and *meso*-BMSE (8.2 mg, 0.053 mmol) with 0.5 mL pyridine to 80 °C for 5 h in a glass tube without stirring. Satisfactory elemental analysis could not be obtained because the compound loses parts of the coordinated pyridine during prolonged drying in vacuo. IR (KBr-pellet): 443 (m), 664 (m), 706 (m), 767 (m), 959 (m), 972 (m), 1067 (vs, ν_{SO}), 1091 (vs, ν_{SO}), 1116 (s), 1438 (w), 1447 (s), 1600 (m), 2911 (m), 2996 (s), 3072 (w). ¹H NMR (400 MHz, 42 °C, DMSO-*d*₆): 3.15 (s, br, 10 H, CH₃ + CH₂CH₂), 7.43 (s, br, 2 H, aryl-*H*_m), 7.85 (s, br, 1 H, aryl-*H*_p), 8.75 (s, br, aryl-*H*_o). ¹H NMR (400 MHz, 93 °C, DMSO-*d*₆): 2.98 (s, br, 3 H, CH₃), 3.10 (s, br, 3 H, CH₃), 3.30 (s, br, 4 H, CH₂CH₂), 7.35 (t, 2 H, ³J_{HH} = 6.9 Hz, aryl-*H*_m), 7.77 (t, 1 H, ³J_{HH} = 7.2 Hz, aryl-*H*_p), 8.60 (s, br, 2 H, aryl-*H*_o).

[Ir(BTSE)(pyridine)₂][PF₆] (12). In an NMR tube, [Ir(BTSE)₂][PF₆] (30 mg, 0.037 mmol) was dissolved in 0.5 mL acetone-*d*₆ and pyridine (5.94 μL) was added. The reaction solution was heated overnight to 45 °C. The NMR spectrum of the reaction solution shows quantitative formation of **12** and 1 equiv of the noncoordinated BTSE. No reaction with water took place. At room temperature, the signals of the pyridine ligands are very broad, due to free rotation of the pyridine. The signals are sharp at -18 °C. ¹H NMR (500 MHz, -18 °C, acetone-*d*₆): δ = 1.27 (s, 18 H, C(CH₃)₃), 2.45 (m, 2 H, CH₂), 4.07 (m, 2 H, CH₂), 7.50 (t, 2 H, ³J_{HH} = 6.3 Hz, aryl-*H*₅), 7.79 (t, 2 H, ³J_{HH} = 6.5 Hz, aryl-*H*₃), 8.15 (tt, 2 H, ³J_{HH} = 7.7 Hz, ⁴J_{HH} = 1.5 Hz, aryl-*H*₄), 8.25 (d, 2 H, ³J_{HH} = 5.6 Hz, aryl-*H*₂), 9.23 (d, 2 H, ³J_{HH} = 5.4 Hz, aryl-*H*₆). ¹³C{¹H}-NMR (126 MHz, -18 °C, acetone-*d*₆): 23.50 (C(CH₃)₃), 54.88 (CH₂CH₂), 66.06 (C(CH₃)₃), 127.14 (aryl-*C*₅), 127.75 (aryl-*C*₃), 141.27 (aryl-*C*₄), 152.84 (aryl-*C*₂), 155.40 (aryl-*C*₆). ³¹P{¹H}-NMR (202 MHz, 25 °C, acetone-*d*₆): -144.7 (sept, 1 P, ¹J_{FP} = 707.4 Hz, PF₆⁻).

[Ir(BTSE)(α-picoline)₂][PF₆] (13). [Ir(BTSE)₂][PF₆] (30 mg, 0.037 mmol) was dissolved in 1.5 mL acetone and α-picoline (10.0 μL) was added at room temperature. The reaction solution was stirred overnight and 5 mL Et₂O was added. The yellow precipitate was filtered off, washed with 2 × 2 mL Et₂O and dried in vacuo to yield 22.0 mg (78.0%) of a yellow powder. ESI/MS *m/z* (%): 618.20 (100) [Ir(BTSE)(α-picolin)₂]⁺, 145.17 (100) [PF₆]⁻. IR: 686 (m), 723 (m), 843 (vs, ν_{PF}), 1064 (s, ν_{SO}), 1106 (m), 1166 (m), 1302 (w), 1362 (w), 1387 (w), 1480 (m), 2868 (w), 2970 (m), 3072 (w). ¹H NMR (500 MHz, 25 °C, acetone-*d*₆): 1.31 (s, 18 H, C(CH₃)₃), 2.51 (s, 6 H, aryl-CH₃), 2.53 (m, 2 H, CH₂CH₂), 3.96 (m, 2 H, CH₂CH₂), 7.48 (d, 2 H, ³J_{HH} = 7.8 Hz, aryl-*H*₃), 7.55 (t, 2 H, ³J_{HH} = 7.2 Hz, aryl-*H*₅), 8.00 (dt, 2 H, ³J_{HH} = 7.8 Hz, ⁴J_{HH} = 1.7 Hz, aryl-*H*₄), 9.38 (dd, 3 H, ³J_{HH} = 6.0 Hz, ⁴J_{HH} = 1.3 Hz, aryl-*H*₆). ¹³C{¹H}-NMR (126 MHz, 25 °C, acetone-*d*₆): = 22.6 (C(CH₃)₃), 22.9 (aryl-CH₃), 53.7 (CH₂CH₃), 64.6 (C(CH₃)₃) 122.3 (aryl-*C*₃), 127.4 (aryl-*C*₅), 139.3 (aryl-*C*₄), 155.9 (aryl-*C*₆), 161.2 (aryl-*C*₂). ³¹P{¹H}-NMR (202 MHz, 25 °C, acetone-*d*₆): -144.3 (sept, 1 P, ¹J_{FP} = 707.3 Hz, PF₆).

[Rh(BTSE)(1,10-phenanthroline)][PF₆] (14). [Rh(BTSE)₂][PF₆] (30.0 mg, 0.041 mmol) and 1,10-phenanthroline (7.4 mg, 0.041 mmol) were dissolved in 1.5 mL CH₂Cl₂ and the reaction mixture

was stirred at room temperature for 3 h. After the reaction, additional 2 mL CH₂Cl₂ were added and all insoluble material was removed by filtration over cotton/celite. Eighteen mL pentane were added to the filtrate forming an orange precipitate which was isolated by filtration, washed with 2 × 3 mL pentane, and dried in vacuo to yield 23 mg (84.8%) of an orange powder. Crystals suitable for X-ray diffraction can be obtained at room temperature by layering a CH₂Cl₂-solution with pentane. Elemental analysis: Calcd. (%) for C₂₂H₃₀S₂O₂N₂PF₆Rh (666.49 g/mol): C 39.65, H 4.54, N 4.20; found: C 40.66, H 4.46, N 4.16. ESI/MS *m/z* (%): 521.68 (100) [Rh(BTSE)(1,10-phenanthroline)]⁺, 145.11 (100) [PF₆]⁻. IR: 721 (m), 844 (vs, ν_{P-F}), 1029 (m), 1078 (s, ν_{SO}), 1152 (w), 1214 (w), 1262 (w), 1351 (m), 1434 (m), 1461 (w), 1515 (w), 1577 (w), 1707 (m), 2860 (w), 2914(w), 2969 (m), 3079 (w). ¹H NMR (500 MHz, 25 °C, CD₂Cl₂): δ = 1.61 (s, 18 H, C(CH₃)₃), 2.54 (m, 2 H, CH₂CH₂), 4.10 (m, 2 H, CH₂CH₂), 8.02 (m, 2 H, aryl-H), 8.14 (s, 2 H, aryl-H), 8.72 (dd, 2 H, ³J_{HH} = 8.0 Hz, ⁴J_{HH} = 1.2 Hz, aryl-H), 9.70 (m, 2 H, aryl-H). ¹³C NMR (101 MHz, 25 °C, CD₂Cl₂): δ = 24.6 (C(CH₃)₃), 50.8 (d, ²J_{RhC} = 2.5 Hz, CH₂CH₂), 67.4 (C(CH₃)₃), 125.6 (aryl-C), 127.5 (aryl-C), 130.2 (aryl-C), 139.5 (aryl-C), 153.0 (aryl-C). ³¹P{¹H}-NMR (101 MHz, 25 °C, CD₂Cl₂): δ = -143.9 (sept, 1 P, ¹J_{FP} = 710.2 Hz, PF₆). UV-vis: λ_{max} , nm ($\epsilon \times 10^{-4}$, M⁻¹cm⁻¹): 227 (3.9), 270 (2.5), 374 (0.6), 463 (0.1).

Crystal Structure Determination of [Rh₂(BTSE)₂Cl₂] 1, [Ir₂(BTSE)₂Cl₂] 2, [Rh(BTSE)₂][PF₆] 3, [Ir(BTSE)(2-methyl-6-pyridinemethanol)(Cl)] 5, [Ir(BTSE)(2-isopropoxy-pyridine)-(H)(Cl)] 7, [Rh(BMSE)(pyridine)(Cl)] 11, and [Rh(BTSE)(1,10-phenanthroline)][PF₆]. Crystal data collection and processing parameter are given in Table 1. Crystals were immersed in a film of perfluoropolyether oil on a glass fiber and transferred to a Nonius

Kappa CCD Diffractometer (Mo K α radiation; **1**, **3**, **5**, **7**, **11**) equipped with an Oxford Cryosystems low-temperature device or a STOE IPDS I image plate diffractometer (Mo K α radiation; **2**, **11**) equipped with a FTS AirJet low temperature device. Data were collected at 120 K (**1**, **3**, **5**, **7**, **11**) or 200 K (**2**, **11**); equivalent reflections were merged and the image were processed with the *Denzo-Scalepack* or the *STOE IPDS* or *CCD* software package. Corrections for Lorentz polarization effects and absorptions were performed and the structures were solved by direct or patterson method. Subsequent difference Fourier syntheses revealed the position of all other non-hydrogen atom and hydrogen atoms were included in calculated positions (except the hydride ligand in **8**, which was free refined). Extinction corrections were applied as required. Crystallographic calculation were performed using *SHELXS-97* and *SHELXL-97*.³⁵

Acknowledgment. This work was supported by the DIP program for German-Israeli Cooperation and by the Minerva Foundation. T.S. gratefully acknowledges the Minerva Foundation (Munich) for a Feodor-Lynen-Postdoctoral Fellowship. D.M. is the Israel Matz Professor of Organic Chemistry.

Supporting Information Available: CIF files containing X-ray crystallographic data for **1**, **2**, **3**, **5**, **7**, **11**, and **14** as well as drawings of the crystal packing of **14**. This material is available free of charge via the Internet at <http://pubs.acs.org>.

IC800354Q